Sādhanā (2020)45:129
https://doi.org/10.1007/s12046-020-01369-3

Investigation of mechanical properties and hot corrosion behavior of friction welded AISI 304 and AISI 1021 steels

AMIT HANDA* and VIKAS CHAWLA

I.K. Gujral Punjab Technical University, Kapurthala, India
e-mail: handaamit2002@gmail.com

MS received 13 July 2019; revised 29 January 2020; accepted 12 February 2020

Abstract. In the current study, friction welding of two different steels, namely low alloy steel and austenitic stainless steel was done. For conducting welding, an in-house experimental set-up was designed and fabricated. The steels were friction welded by using various axial pressures at a uniform circular speed. Influence of axial pressure on the joint strength of the friction welded specimens such as tension, impact toughness, torsion strength and microhardness were evaluated. Moreover, the weldments were also tested for high temperature corrosion resistance. The corrosion testing of the welded joints was carried out in a molten salt environment of $Na_2SO_4 + V_2O_5$ 60% at 650°C. Weight change data were used to establish the kinetics of corrosion. Based upon this data, the weldments showing best corrosion resistance was identified. Subsequently to understand the composition of oxide scale, the specimen was evaluated using SEM/EDS and X-ray diffraction techniques.

Keywords. Friction welding; dissimilar metals; mechanical testing; hot corrosion; molten salt environment.

1. Introduction

In several industries, there is a need to weld austenitic and ferritic steel to achieve special combinations of properties, for instance, in power generation industry [1]. However, several metallurgical and fabrication limitations arise while joining dissimilar materials, which can lead to in-service failures [2, 3]. The most noticeable welding defects are hot cracks attributed to unintended application of improper C-steel electrodes [4]. Using these electrodes may also lead to the development of extremely hard, crack-pronounced structure towards the stainless-steel side of the dissimilar weldments, whereas interrupted hard and brittle zones along the interface line of ferrite side of weldment [4]. These brittle and hard regions may lead to oxidation attack, localized pitting and failure of the joint due to uneven stresses. Numerous industrial failures are reported within the open literature [4]. Moreover, while studying the literature it has been noticed that in the power generating equipment, high temperature oxidation is a very thoughtful concern which can lead to in-process failures [5–8]. High temperature corrosion is the enhanced corrosion of metals at high temperatures, aggravated by the fluxing of fused salt on the metal surfaces. The need of hot corrosion has aroused as during welding dissimilar materials, different cooling rates were observed [9] and these led to the formation of corrosive layer at the interface with the passage of time and the joint gets failed. It has been concluded from the literature that most of such failures occur in the weldment region [4]. Therefore, there is a need to investigate the problem to a greater depth. Moreover, it is learnt that no work has been done to investigate the high temperature corrosive behavior of friction weldments AISI 304/AISI 1021 steels.

In the present investigation, a friction welding set-up was fabricated and retrofitted on a heavy-duty conventional lathe for the fabrication of friction weldments. Subsequently, an attempt was made to evaluate the joint behavior of the friction weldments of dissimilar steels, produced by changing the axial pressures at a fixed rotational speed. Furthermore, the performance of the produced friction welded joint was evaluated in a corrosive atmosphere; consisting of an eutectic mixture of Na_2SO_4-V_2O_5 60% at 650°C under cyclic conditions. The combinations of ferritic and austenitic steels are commonly applicable in fabricating boiler tubes, owing to their good mechanical properties along with economy [1]. However, such weldments are usually exposed to serious hot corrosion problems [10].

2. Experimental procedure

2.1 *Experimental set-up*

In the current investigation, weldments of AISI 1021 and 304 steels were made using an in-house developed continuous drive friction welding machine. Figure 1 presents the custom-made friction welding set-up. The experimental

*For correspondence
Published online: 16 May 2020

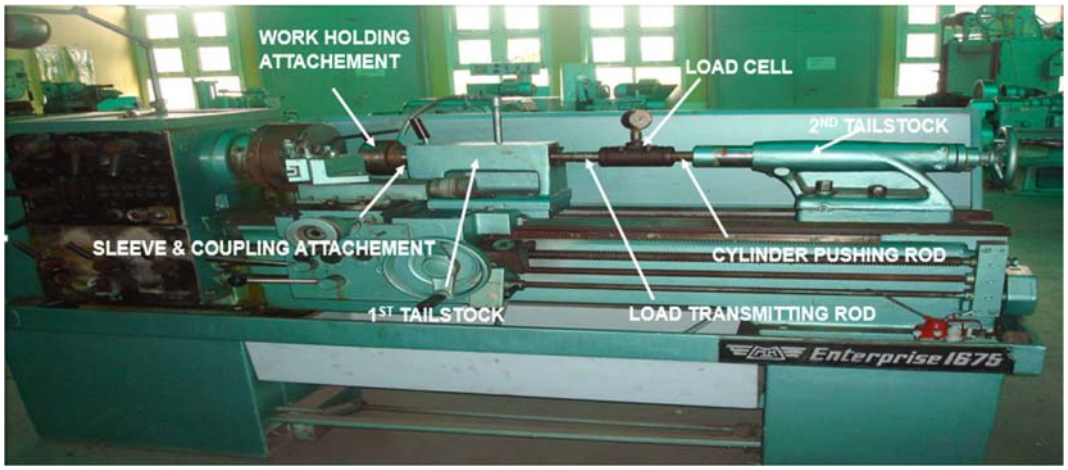

Figure 1. Custom made friction welding set-up.

set-up consisted a heavy-duty lathe (Kirloskar, MK 1675), which was employed for friction welding; after incorporating suitable modifications on it. To monitor axial pressure generated at the weld interface, a loading device was fabricated and installed between the tailstocks. A master brake cylinder was used in the loading device and DOT-4 oil was used inside the fabricated load cell to transmit the power. For evaluating the axial pressure, a pressure gauge was attached on the brake cylinder having the measuring capability ranging from 0–150 MPa. Cylinder pushing and load transmitting rods were used to transmit the power.

In the present work, the test material used were AISI 1021 low alloy steel and AISI 304 austenitic stainless steel; the actual and nominal chemical composition of the investigated metals are reported in table 1. Table 2 reports the actual mechanical properties of the base metals.

Cylinder bars (specimens), measuring 20 mm in diameter and 100 mm length, were prepared from bars of steels. Subsequently, these bars were fitted on the friction welding machine. AISI 304 steel specimen was kept fixed, whereas AISI 1021 steel specimen was rotating during the start of welding cycle. For maintaining the reliability and repeatability of the experiment three samples were produced at each and every parameter and their average values were taken.

All the weldments were prepared at a constant rotational speed of 1430 rpm, using five different axial pressures in a range of 75 MPa to 135 MPa in the graduations of 15 MPa. These welding parameters were adopted from the literature and as the basis of some pilot experiments [11].

2.2 *Evaluation of mechanical properties*

Evaluation of mechanical properties of the fabricated welds was done so as to establish their appropriateness for the expected service life. UTM with capacity of 60T was used for performing the tensile testing. During this testing, the friction welded samples were tested to gradually increasing tensile load until their fracture occurred. A370-12 ASTM standards were followed to prepare all the tensile test specimens. Torsion test was done on a torsion testing machine (Scientific Instruments Limited). In this test, twisting moment was applied on the specimens till their fracture occurred. Angle of twist along with applied torque were measured during the testing. To evaluate the notch impact toughness, a pendulum type single blow impact testing machine was used. The specimens were prepared as per A370-12 ASTM standards, keeping notch on the weld bead. Prepared samples were fitted in a simply supported beam configuration (Charpy test) in the anvil of the machine. Subsequently, the specimens were subjected to impact load by a free-falling hammer and the absorbed energy by the weldments to fracture were recorded. Izod

Table 1. Chemical composition of the base metals.

	Metal	Cr	Ni	C	Mn	Si	P	S	Fe
Nominal Composition	AISI 1021	–	–	0.15–0.25	0.6–0.9	–	–	–	Bal.
Actual Composition	AISI 1021	0.00	0.00	0.22	0.68	0.23	0.04	0.04	Bal.
Nominal Composition	AISI 304	17-20	9-13	0.08	2	0.75	–	–	Bal.
Actual Composition	AISI 304	17.35	10.24	0.04	1.88	0.78	0.02	0.02	Bal.

Table 2. Mechanical properties of the base metals actually tested under standard conditions.

Metal	Tensile Strength	Impact Strength (Charpy)	Impact Strength (Izod)	Microhardness
AISI 1021	473MPa	126 J	96 J	188 Hv
AISI 304	529MPa	138 J	104 J	202 Hv

impact test was also conducted in which the samples were vertically placed as a cantilever with the notch facing towards dropping pendulum. A Vicker hardness testing machine was used for evaluating the micro hardness values. A pyramid type diamond indenter with square base was used in this test under a load of 500 gf for a dwell period 10 s. The variation in hardness along the joint interface (weld bead) and along both the base metals was evaluated at regular intervals of 1 mm.

2.3 *Hot corrosion test*

For performing hot corrosion test, the friction welded specimens, which were initially cylindrical shaped, were cut into rectangular coupons of size 20 × 15 × 5 mm by wire-cut EDM, keeping the welded area at the center of specimen. Figure 2 presents the prepared samples for hot corrosion study. Before the corrosion run, all samples were polished down to mirror finish as per the standard metallurgical procedure. After polishing, the samples were preheated to 250°C and immediately a coating having 3–5 mg/cm^2 of salt mixture of Na_2SO_4–V_2O_5 60%was coated with a camel hair brush. Cyclic studies were conducted on these specimens for 50 cycles. Every cycle contained the heating of specimen for 60 minutes at 650°C in a SiC tube furnace followed by 20 minutes of cooling at ambient temperature. At the end of each cycle, weight gain measurements were done using a digital weighing machine having a sensitivity of 1 mg. The specimens were heated by keeping one sample at a time in alumina boat so that the spalled scale, if any, could be collected in the boat and included in weight change measurements. This was done to evaluate the total rate of corrosion. XRD and SEM/EDS analyses were done to characterize the oxide scales at different locations on each of corroded sample.

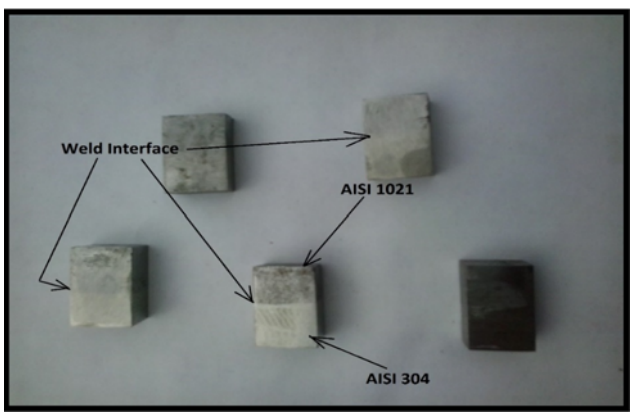

Figure 2. Produced samples from cylindrical weldments used for hot corrosion study.

3. Results and discussion

3.1 *Tensile test*

During testing, it has been found that tensile strength varied in the range from 405 MPa to 481 MPa, whereas the strain values ranged from 0.2279 to 0.4403 based on the axial pressure used. Average tensile strength and standard deviation data is compiled in table 3. These values are in good agreement with those quoted by Arivazhagan *et al* [12]. Variation of stress with strain has been reported in figure 3. It can be seen from the figure that the specimen produced at 120 MPa axial pressure has shown a maximum ductility.

Moreover, in all the cases, the strain is found to increase with the increase in stress in initial stages of testing. Subsequently, the stress starts decreasing after achieving the maximum value, however the strain uninterruptedly upsurges till the failure occurs. Similar behavior has also been reported by Ozdemir [13]. After tensile testing, SEM analysis conducted at the fractured locations, which was compiled in figures 4(a)-(e). It can be observed from the fractographs that the cleavage fracture and river like patterns [14] are observed for 75 MPa (figure 4(a)) axial pressure sample. These features are characteristic of brittle fracture. Quasi-cleavage fracture could be found for the 90 MPa sample [14] presented in figure 4(b), indicating that the failure might have happened by the mixed phenomenon. Dimpled patterns are seen for the 105 MPa axial pressure sample (figure 4(c)), indicating that the failure may have taken place by a ductile manner [14]. The fractographs for the 120 MPa and 135 MPa samples reveal that dimples are deep compared to 105 MPa showing relatively higher ductility. Visual inspection of the fractured specimens also shows that brittle fracture occurred for the 75 MPa and 90 MPa axial pressure samples and the joints failed at welding joint, while ductile failures were noticed for the samples prepared at 105 MPa (figure 4c), 120 MPa (figure 4(d)) and 135 MPa (figure 4(e)) pressures. The joint strength of these three latter produced samples were observed to be almost equal to the strength in tension of the weaker base metal, which is AISI 1021. Based on the rise in pressures,

Table 3. The average tensile and torsional strength data along with standard deviation for the friction weldments fabricated at 1430rpm using different axial pressures.

Specimen	Axial Pressure (MPa) for Friction Welding	Average Tensile Strength (MPa) and Standard Deviation	Average Torque (Nm) and Standard Deviation
A 1	75	405 ± 19.79	18.14 ± 0.90
A 2	90	429 ± 25.28	23.53 ± 1.20
A 3	105	464 ± 26.76	24.51 ± 1.15
A 4	120	481 ± 18.38	36.77 ± 1.66
A 5	135	467 ± 16.97	34.32 ± 1.65

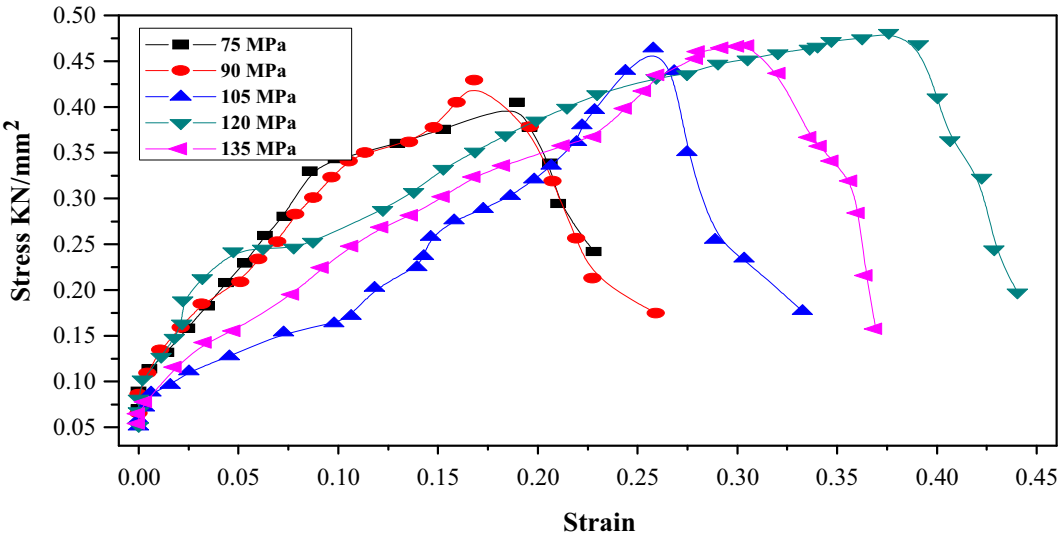

Figure 3. Relationship between stress and strain for friction welded AISI 304 and AISI 1021 steel samples.

additional mass is believed to be flashed out owing to more friction, thereby enhancing the joint strength.

The plot between percentage elongation and peak tensile loads (KN) is shown in figure 5, which shows that percentage elongation is increasing with increase in load till the axial pressure of 120 MPa, beyond which the same starts decreasing. This decline in percentage elongation may be attributed to the formation of inter-metallic compounds of brittle nature at the weld interface, which may have been produced due to higher axial pressures leading to the generation of higher temperatures [15]. A similar occurrence has been observed while friction welding of dissimilar metals by Handa and Chawla [16] and Yilmaz *et al* [15]. The specimen produced at 120MPa exhibited the highest tensile strength among the investigated cases along with a maximum percentage elongation of 1.8%, which is more than the AISI 1021 base metal. It is believed that with the rise in pressures, the higher concentration elements of austenitic stainless-steel starts migrating towards the low alloy steel, thereby enhancing the ductility and the strength of the weldment.

3.2 *Torsion test*

Average torque and standard deviation results for the frictionally joined samples are presented in table 3. During experimentation it was noticed that the torsional strength and the angle of twist were varied from 18.14 Nm to 36.77 Nm and 9° to 28°, respectively. However, all the samples were failed from the weld interface. Similar findings have been quoted by Shribman *et al* [17] and Shribman [18]. Figure 6 depicts the variation of the torque with angle of twist, which indicates that the angle of twist increased with the increase in torque, which is as per the expectations. It has also been noticed that the angle of twist and torsional strength both directly influenced with the increase in axial pressures. Again, this might be the result of diffusion of high concentration elements from austenitic SS to ferritic steel [17, 18]. However, as the pressure was raised past 120 MPa during welding, there was a marginal drop in the torque. The maximum available torque and angle of twist was 36.77 Nm and 28° for the specimens fabricated at 120 MPa axial pressures. It is pertinent to mention that the same sample showed best results during tensile testing.

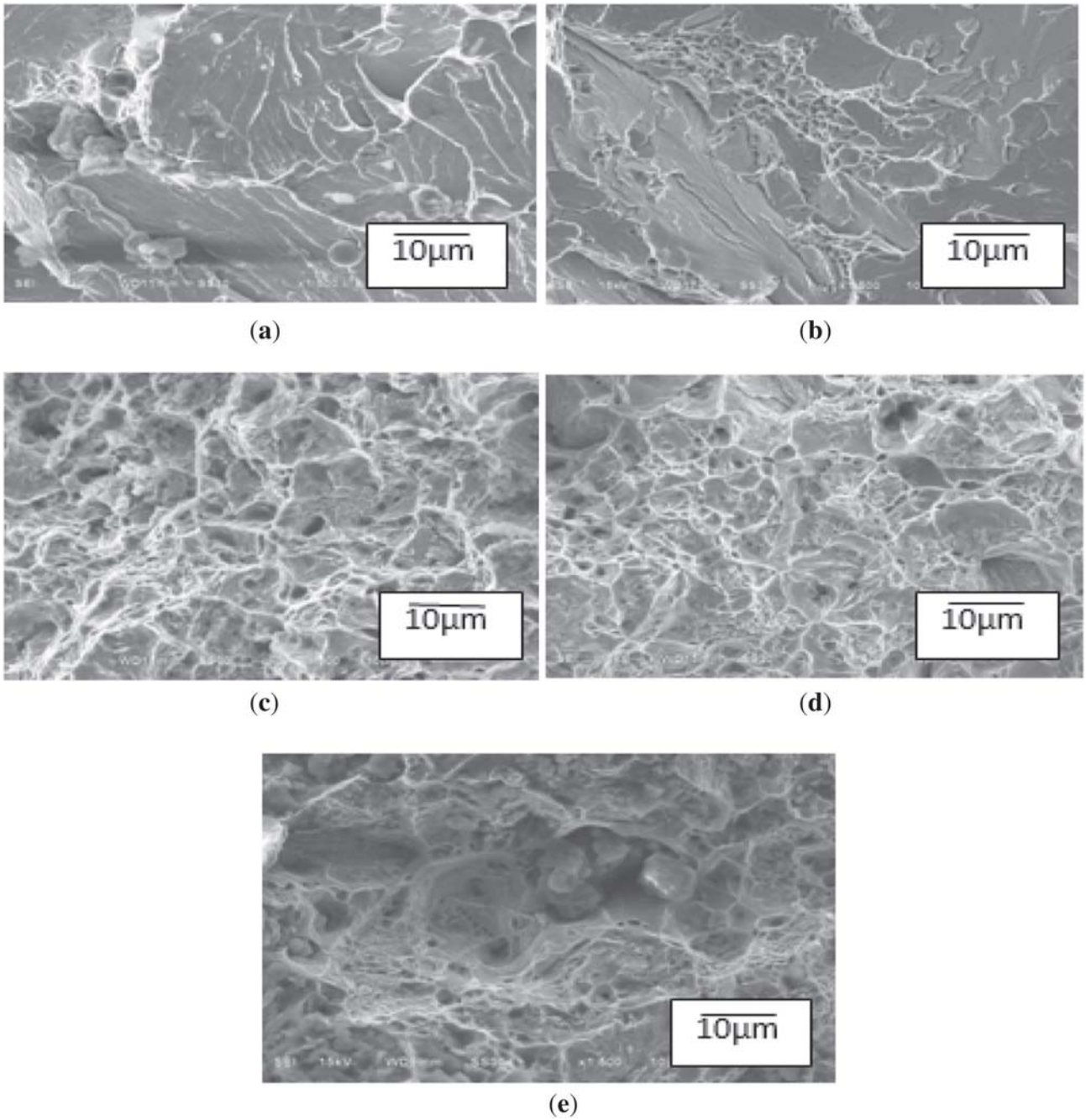

Figure 4. SEM fractographs of friction welded AISI 304 and AISI 1021 steel samples failed under tensile testing. The samples were prepared at several axial pressures (a) 75 MPa, (b) 90 MPa, (c) 105 MPa, (d) 120 MPa and (e) 135 MPa.

3.3 *Impact test*

The results of both the Charpy as well as Izod impact tests presented in figure 7. It could be observed from the figure that the Charpy toughness of the weldments, in general, is somewhat greater than that of the Izod impact toughness, which is attributable to the different loading configuration of the specimens in both the tests. The recorded results after experimentation are in good agreement with that of open literature [19, 20]. It could be observed that the impact strength of the weldment was influenced by the burn-off length. The lower burn-off length gives the maximum impact strength of both Izod and Charpy tests, whereas the lowest strength values were monitored at uppermost burn-off lengths. The obtained results are quite comparable with those reported in the literature [4, 12]. The decrease in toughness values with the increase in burn-off length might be attributed to the relocation of carbon from the AISI 1021 to AISI 304 due to higher temperatures, which prevail at the joint interface section [4]. Moreover, higher temperatures

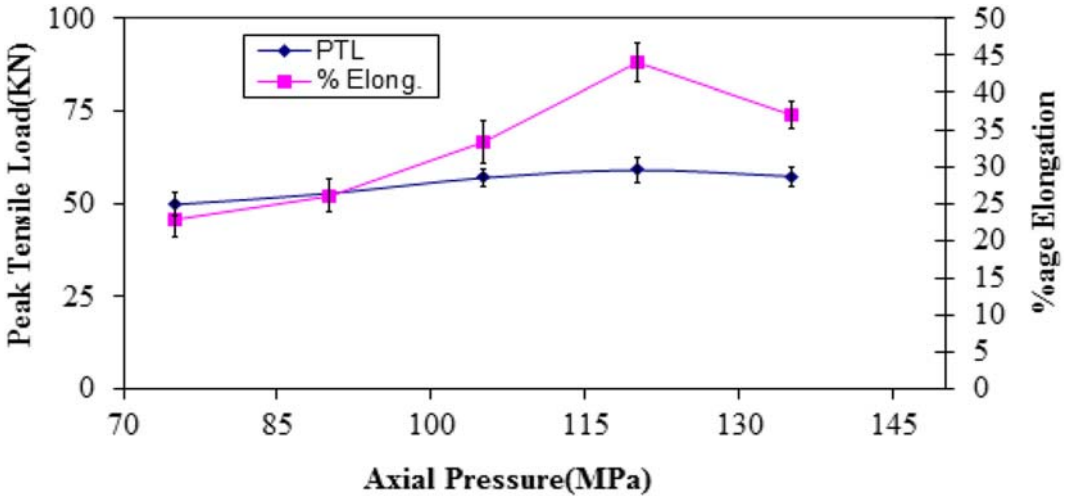

Figure 5. Relationship between average peak tensile load and %age elongation for friction welded AISI 304 and AISI 1021 steel samples subjected to tensile tests.

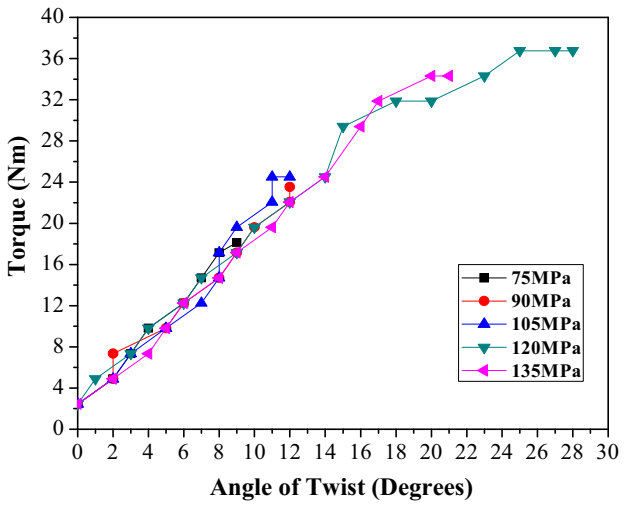

Figure 6. Relationship between torque and angle of twist for friction welded AISI 304 and AISI 1021 steel samples subjected to torsion tests.

are attained in very short times under high friction force conditions as contrary to low friction circumstances [21]. Under these conditions, peak temperature input rates and lower welding times might result in prompt cooling of the material [21].

3.4 *Microhardness*

The hardness data for the investigated cases is reported in figure 8. AISI 1021 is found to have lesser hardness in comparison to austenitic stainless steel. This decline in hardness values might be attributed to the recrystallization process that might have taken place in the heat affected zone towards AISI 1021 steel [22]. It has also been noticed in all the weldments that the maximum hardness values were attained at the welded region, similar to observations of Ozdemir and Orhan [23]. It has been pertinent to mention that the hardness gradually decreases as we move away from the 0-line towards the either base metal. However, the maximum hardness values have been noticed at weld interface region. Due to higher heat input conditions, higher temperatures are attained in shorter times. Subsequently the dissipation rate of the generated heat also rapidly increased, leading to the formation of martensite and compressed zone at the weld interface [21]. Figure 9 depicts the formation of martensite at the weld region and highly compressed zone leading to increased hardness values at the weld interface. Moreover, it was anticipated that a soft region appears towards AISI 304 side with the increase in burn-off length. The establishment of this softer zone could be attributed to decarburization. As the conductivity of the metal is comparatively low, so this might have happened due to the occurrence of heat at the joint interface [19]. The peak values of hardness at the welded joints are perhaps due to the oxidation process which may take place during the friction welding [24]. For all samples, relatively higher hardness was noticed towards AISI 304 steel side, which may be due to the fact that AISI 304 steel having much lower thermal conductivity in contrast to AISI 1021 steel [25, 26].

3.5 *Visual examination of the hot corroded samples*

After the very first cycle of hot corrosion, the welded specimen was found to have rough scale with light brown patches. The number of patches were more on the low alloy steel side, that is, towards AISI 1021. The number of patches started increasing after the third cycle and the colour

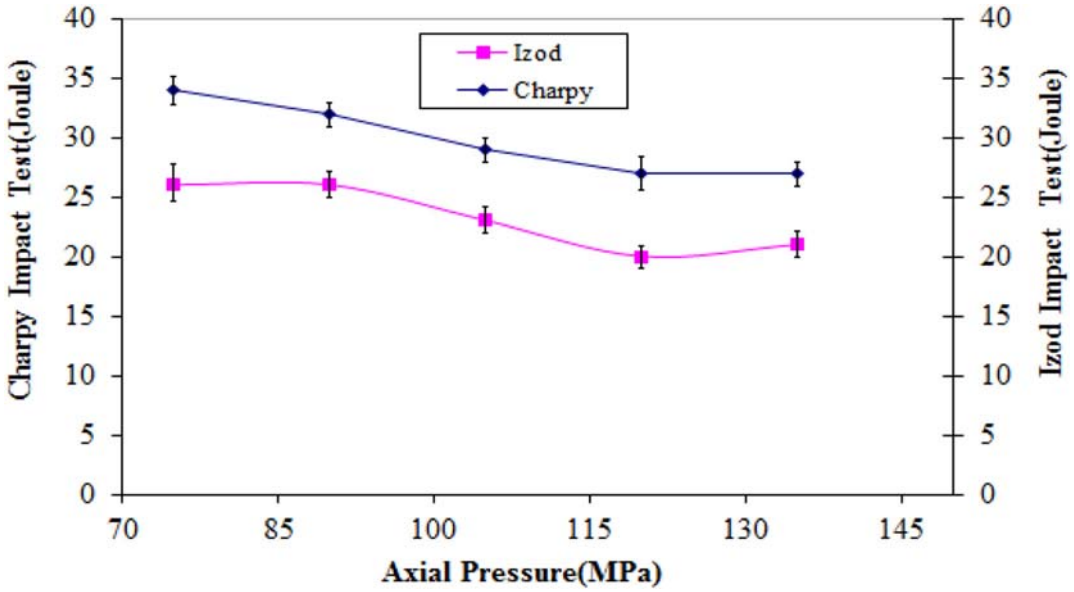

Figure 7. Relationship between average impact toughness and axial pressure for friction welded AISI 304 and AISI 1021 steel samples subjected to impact tests.

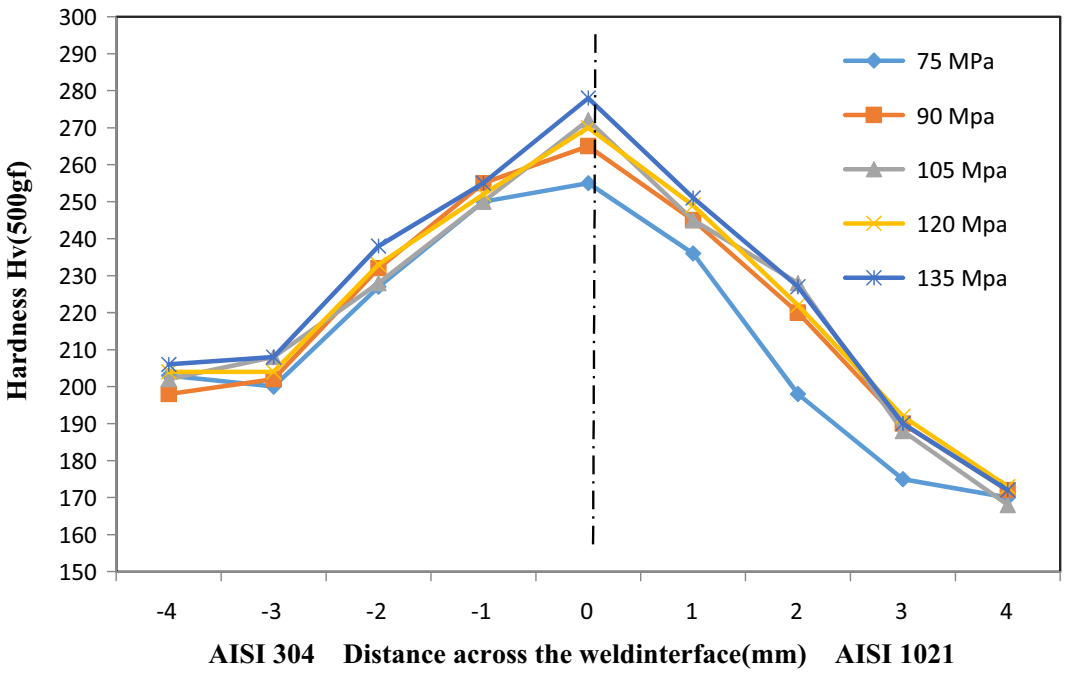

Figure 8. Variation of hardness across the weld interface for friction welded AISI 304 and AISI 1021 steel samples subjected to micro hardness testing.

of the patches turned into brown. After the end of 8th cycle, the scale became thicker and the colour was changed to dark brown on the AISI 1021 steel side, while on AISI 304 steel side, the colour was converted to silvery grey. With the additional growth in number of cycles the scale became darker. Colour of the scale at the joint interface was observed to be totally changed from that of parent materials. After 17th cycle, extent of spalling got increased; subsequently extensive spalling was observed. Figure 10 presents the hot corroded sample after 50 cycles of exposure.

3.6 *Weight change data*

The plots of cumulative weight gain (mg/cm^2) as the function of time in terms of number of cycles for the investigated weldments subjected to hot corrosion at a

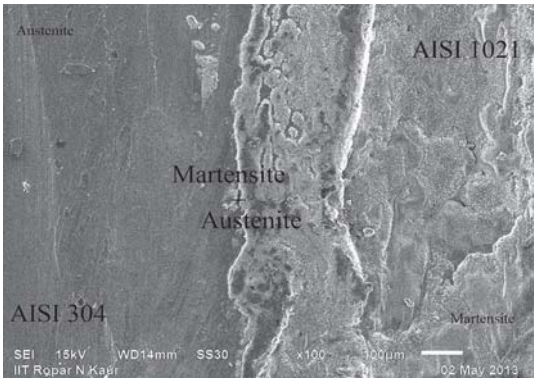

Figure 9. Depicts the formation of martensite and highly compressed zone at the weld interface.

temperature of 650°C in $Na_2SO_4 + 60\%\ V_2O_5$ environment up to 50 cycles are shown in figure 11. Among the weldments, a maximum cumulative weight gain was recorded for the specimen, fabricated at 90 MPa axial pressure, whereas a minimum, for those made at 120 MPa and 135 MPa axial pressures. Considering the parent metal, the maximum cumulative gain was recorded for AISI 1021, which was found to be 14.2 mg/cm^2. This was more than the weight gain observed for the samples fabricated at 90 MPa. A minimum value was observed for AISI 304 as 9.4 mg/cm^2, which was less than that observed for 120 MPa and 135 MPa cases. As per the hot corrosion weight gain graph, somewhat oscillation type reaction weight gain rate has been noticed for all the cases, maybe owing to change in reaction rate, which are related with the development of laminated inner oxide layer as advised by Hurdus *et al* [27]. After completion of 50th cycle of hot corrosion, it is obvious from Figure 10 that the effect of hot corrosion is more on AISI 1021 side, which was also

Figure 10. Macrograph of a friction welded AISI 304 and AISI 1021 steel sample, prepared at 1430 rpm and 120 MPa axial pressure, subjected to hot corrosion testing in $Na_2SO_4 + V_2O_5$ 60% environment for 50 cycles at 650°C.

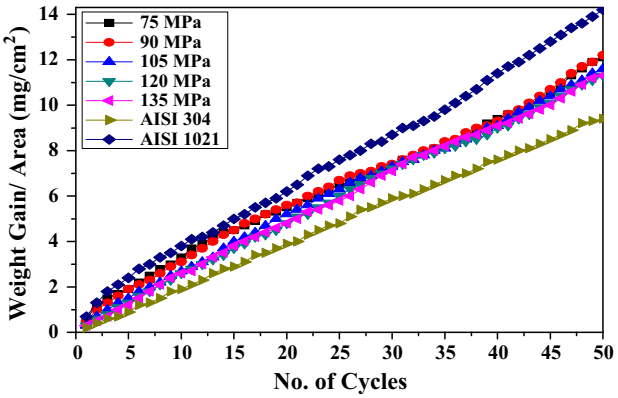

Figure 11. Cumulative weight gain graph of both the parent metals as well as friction welded samples prepared at different axial pressures.

perceptible from the degree of observed spalling of the scale from this side.

3.7 *SEM/EDS and XRD analysis*

SEM images of friction welded specimens presenting surface morphology after cyclic hot corrosion for 50 cycles at 650°C are presented in figure 12. The images of corroded samples clearly point out the tendency for spalling of the scales. The analysis was done on the weld joint and up to a distance of 3mm on either side of the weldment at regular intervals of 1mm, therefore capturing seven SEM images on the sample. The EDS analysis depicts the existence of Fe and O as the predominant elements in all cases in general, along with small amounts of Cr, Ni and Mn. This indicates the formation of iron-oxide rich oxide layer. The noticed severe spalling of the scales was attributed to the intensive strain produced owing to the precipitation from the liquid phase of Fe_2O_3 and the inter diffusion of intermetallic layers of Fe_2O_3 as has been described by Arivazhagan *et al* [4]. The scale thickness was noticed to be higher on AISI 1021 side than that on AISI 304 side. This scale growth may result into the detachment of scale, which may be due to the result of two-way flow of the reactants [28]. Moreover, while welding dissimilar metals, the coefficients of thermal expansion differ for each of the base metal, weldment, and the scale, therefore additional stresses are produced while cooling, which might have affected adhesion characteristics of the scale leading to spallation.

Furthermore, from the XRD analysis, it is apparent that the corroded welded samples having Fe_2O_3 and Cr_2O_3 as major phases in their oxide scales, along with relatively weak phases of $NiCr_2O_4$, MnO_2 and FeNi. Similar SEM/EDS analysis at other locations has been shown in figure 12 which show similar trends. Similar findings are also reported by Arivazhagan *et al* [1]. The XRD peak intensity is also seen to increase when we move from AISI 304 to

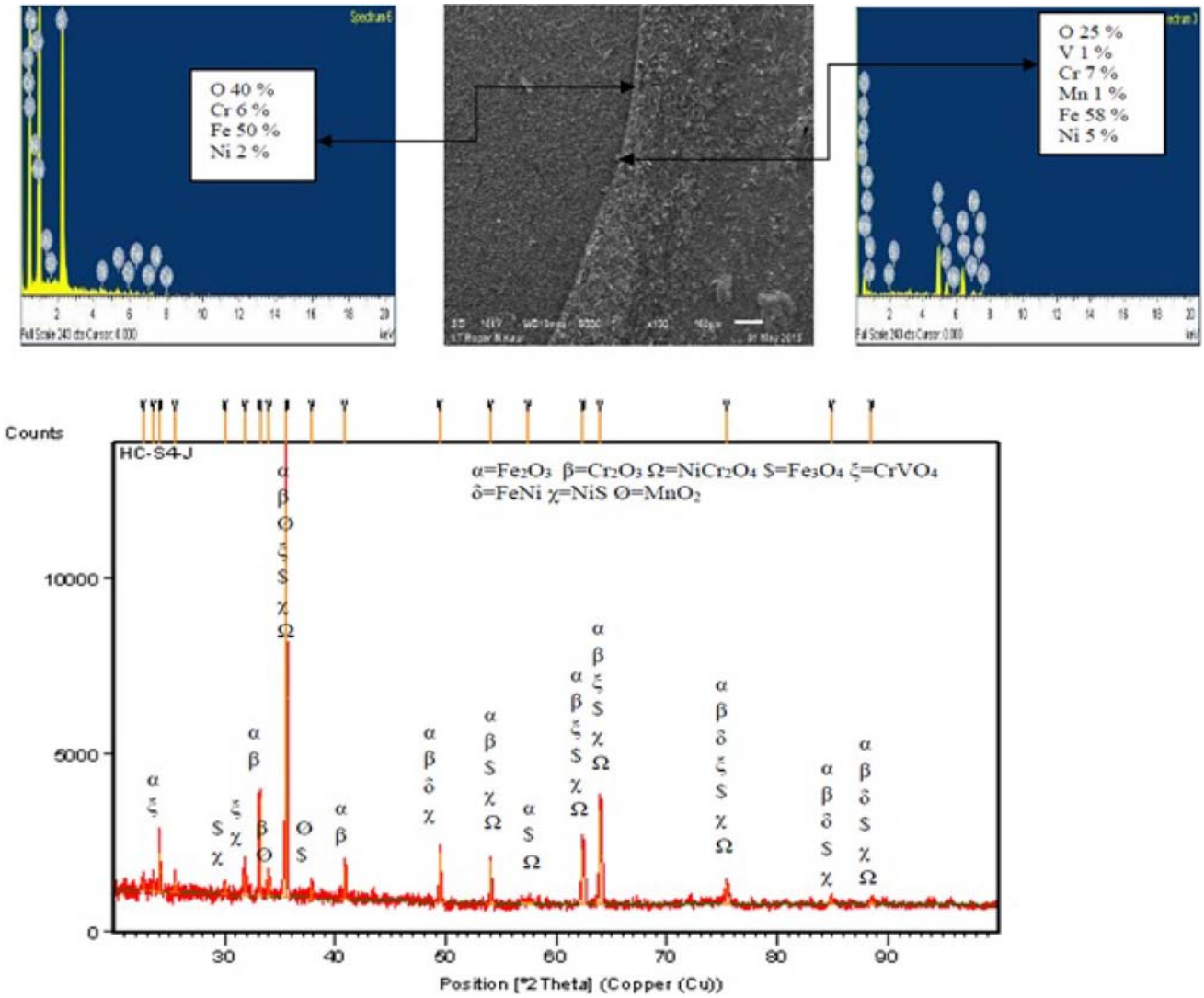

Figure 12. SEM/EDS and XRD analysis of AISI 304 and AISI 1021 steel weldments prepared at 1430 rpm at an axial pressure of 120 MPa.

AISI 1021 zones. Relatively weak peaks of chromium oxide are also seen towards the low alloy steel, suggesting that the Cr might have diffused during friction welding from AISI 304 towards AISI 1021 side. Similar observations have been noticed by many researchers [4]. Existence of Cr in the scale, along with the Fe and O in the hot corroded sample is in good agreement with Sadique *et al* [29].

4. Conclusions

AISI 1021 and 304 steels were effectively joined by friction welding at various axial pressures with different burn-off lengths (5 mm to 11.75 mm). It was found that the generated flash was confined towards ferritic steel, which may be due to the fact that AISI 304 steel have considerably lower thermal conductivity along with higher hardness at elevated temperatures in comparison with low alloy steel. Following conclusions were drawn based on the experimental study.

1. The joint strength in tension of the weldments were noticed to be very close to that of weaker base metal and at 120 MPa pressure it was observed to be 481 MPa slightly higher than the weaker parent metal. In general, it was noticed that the joint strength increases with the rise in axial pressure.
2. It has been concluded that optimized torsional strength in general can be achieved at the same axial pressure i.e., at 120 MPa even though all the specimens failed at the weld interface.
3. It was concluded that hardness increases with the rise in burn-off length, whereas impact toughness follows reverse trend.

4. The weight change data for the weldments indicated the presence of oscillation type reaction rates during hot corrosion, which may be due to spalling of thicker scale on low alloy steel side.
5. The higher content of Cr_2O_3 and Fe_2O_3 in the scale over the joint interface might be owing to enrichment of this region with iron and chromium.
6. From the XRD analysis it could be inferred that as one moves from 304 steel towards 1021 steel through the joint interface, the intensity of Fe_2O_3 phase was higher in the scale on the base 1021, however higher content of Cr_2O_3 was observed on the 304 side, which might be due to the augmentation of this zone with chromium.
7. In general, friction welding technique provides best compromise of joint strength in tension, torsional strength, impact strength, %age elongation, hardness uniformity along with corrosion resistance behavior at an axial pressure of 120 MPa.

References

[1] Arivazhagan N, Singh S, Prakash S and Reddy G M 2006 High temperature corrosion studies on friction-welded dissimilar metals. *Mater Sci Eng* 132: 222–227

[2] Meshram S D, Mohandas T and Reddy G M 2007 Friction welding of dissimilar pure metals. *J Mater Process Technol* 184: 330–337

[3] Handa A and Chawla V 2014 Investigation of mechanical properties of friction welded AISI 304 with AISI 1021 dissimilar steels. *Int J Adv Manuf Technol* 75: 1493–1500

[4] Arivazhagan N, Singh S, Prakash S and Reddy G M 2008 An assessment of hardness, impact strength and hot corrosion behavior of friction-welded dissimilar weldments between AISI 4140 and AISI 304. *Int J Adv Manuf Technol* 39: 679–689

[5] Johnson D M, Whittle D P and Stringer J 1975 Oxidation of Na_2SO_4-coated cobalt base alloys. *Corros Sci* 15: 649–661

[6] Rapp R A 2002 Hot corrosion of materials: a fluxing mechanism? *Corros Sci* 44: 209–221

[7] Fryburg G C, Kohl F J and Stearns C A 1984 Chemical reactions involved in the initiation of hot corrosion of IN-738. *J Electrochem Soc* 131: 2985–2996

[8] Stringer J 1977 Hot corrosion of high-temperature alloys. *Ann Rev Mater Sci* 7: 477–509

[9] Arivarasu M, Manikandan M, Gokulkumar K, Rajkumar V, Devendranath K and Arivazhagan N 2014 High temperature studies on welded joint in molten salt power plant environments. *Int J ChemTech Res* 6: 409–415

[10] Arivazhagan N, Narayanan S, Singh S, Prakash S and Reddy G M 2012 High temperature corrosion studies on friction-welded low alloy steel and stainless steel in air and molten salt environment at 650°C. *Mater Des* 34: 459–468

[11] Sahin M 2009 Characterization of properties in plastically deformed austenitic-stainless steels joined by friction welding. *Mater Des* 30: 135–144

[12] Arivazhagan N, Singh S, Prakash S and Reddy G M 2011 Investigation of AISI 304 austenitic stainless steel to AISI 4140 low alloy steel dissimilar joints by gas tungsten arc, electron beam and friction welding. *Mater Des* 32: 3036–3050

[13] Ozdemir N 2005 Investigation of the mechanical properties of friction welded joints between AISI 304L and 4340 steel as a function rotational speed. *Mater Lett* 59: 2504–2509

[14] ASM Handbook 1987 *Fractography* 12: 43–58

[15] Yilmaz M, Col M and Acet M 2002 Interface properties of aluminum/steel friction welded components. *Mater Charact* 49: 421–429

[16] Handa A and Chawla V 2015 Evaluation of tensile strength and fracture behaviour of friction welded dissimilar steels under different rotational speeds and axial pressures. *Sadhana Acad Proc Eng Sci* 40: 1639–1655

[17] Shribman V, Stern A, Livshitz Y, Gafri O 2002 Magnetic pulse welding produces high strength aluminium welds. *AWS Weld J* 81: 33–37

[18] Shribman V 2008 Magnetic pulse welding for dissimilar and similar materials. In: *3rd International Conference on High Speed Forming*, Dortmund, Germany, pp. 13–22

[19] Satyanarayana V V, Reddy G M and Mohandas T 2005 Dissimilar metal friction welding of austenitic-ferritic stainless steel. *J Mater Process Technol* 160: 128–137

[20] Handa A and Chawla V 2013 Experimental study of mechanical properties of friction welded AISI 1021 steels. *Sadhana Acad Proc Eng Sci* 38: 1407–1419

[21] Chander G S, Reddy G M and Tagore G R N 2012 Influence of process parameters on impact toughness and hardness of dissimilar AISI 4140 and AISI 304 continuous drive friction welds. *Int J Adv Manuf Technol* 64: 1445–1457

[22] Ananthapadmanadan D, Rao V S, Abraham N and Rao K P 2009 A study of mechanical properties of friction welded mild steel to stainless steel joints. *Mater Des* 30: 2642–2646

[23] Ozdemir N and Orhan N 2005 Microstructure and mechanical properties of friction welded joints of a fine-grained hypereutectoid steel with 4% Al. *J Mater Process Technol* 166: 63–70

[24] Ates H, Turker M and Kurt A 2007 Effect of friction pressure on the properties of friction welded MA956 iron-based superalloy. *Mater Des* 28: 948–953

[25] Sammaiah P, Suresh A and Tagore G R N 2010 Mechanical properties of friction welded 6063 aluminum alloy and austenitic stainless steel. *J Mater Sci* 45: 5512–5521

[26] Handa A and Chawla V 2014 Influence of process parameters on torsional strength, impact toughness and hardness of dissimilar AISI 304 and AISI 1021 friction welded steels. *Mater Eng* 21: 94–103

[27] Hurdus M H, Tomlinson L and Titchmarsh J M 1990 Observation of oscillating reaction rates during the isothermal oxidation of ferritic steels. *Oxid Met* 34: 429–464

[28] Atkinson A 1982 Conditions for the formation of new oxide with oxide films growing on metals. *Corros Sci* 22: 347–357

[29] Sadique S E, Mollah A H, Islam M S, Ali M M, Megat H H and Basri S 2000 High temperature oxidation behavior of iron-chromium-aluminum alloys. *Oxidat Met* 54: 385–400